

# Structural bioinformatics: Bridging the gap between 3D structure and function

## Engineering enhanced ligand affinity without additional van der Waals or electrostatic interactions

Finn Bauer<sup>a,b</sup>, Kristian Schweimer<sup>b</sup>, Anke Eisenmann<sup>b</sup>, Paul Rösch<sup>b</sup> and Heinrich Sticht<sup>a</sup>

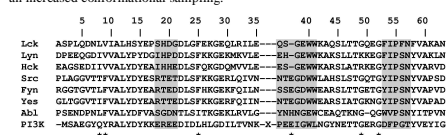
<sup>a</sup> Institut für Biochemie, Abt. Bioinformatik, Emil-Fischer-Zentrum, Universität Erlangen-Nürnberg, 91054 Erlangen, Germany  
<sup>b</sup> Lehrstuhl für Biopolymere, Universität Bayreuth, 95440 Bayreuth, Germany

### Summary

Class II ligands of src homology 3 (SH3) domains are peptides containing the consensus sequence XPPLPKR (where X is any amino acid residue). This peptide forms a left-handed type II polyproline (PPII) helix that lies along the binding site of the SH3 domain, with its prolines interacting with the aromatic residues on the hydrophobic face of the SH3 domain. The flexibility of the ligand binding site comprising the RT loop, the n-src loop and a  $3_{10}$  helix is thought to play a decisive role in determining the binding affinity.

The SH3 domains of the nonreceptor tyrosine kinases Lck and Lyn were chosen to investigate the role of particular residues in the binding interface to understand their role in ligand binding affinity. Both SH3 domains investigated bind with different affinities to a peptide of the herpesviral tyrosine kinase interacting protein (Tip) forming a PPII helix. The fundamental idea was to induce an increased loop flexibility, leading to a rise of conformational sampling and to end up in an increased ligand affinity without altering the van der Waals or electrostatic interaction.

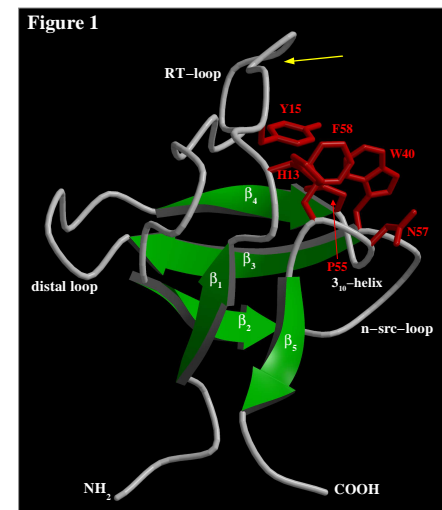
Sequential alignments of LckSH3 and LynSH3 suggested a P to G variation of the RT loop at position 17 to increase loop flexibility. Molecular dynamics calculations anticipate not only a local increase of flexibility of the mutant RT loop, but an increase of flexibility of all three loops of the SH3 domain. Nuclear magnetic resonance (NMR)  $^{15}\text{N}$  relaxation methods have been used to characterize the backbone dynamics of the wild-type and mutant SH3. Variations in the  $\{^1\text{H}\}^{-15}\text{N}$  nuclear Overhauser effects (hetNOE) and the longitudinal ( $R_1$ ) and transverse ( $R_2$ )  $^{15}\text{N}$  backbone amide relaxation rates for individual amino acids correlate with the degree of atomic fluctuation extracted from the MD simulations. Finally, the binding affinity was determined by fluorescence spectroscopy, revealing an 8-fold increase of the  $K_D$  of the P17G mutant compared with wild-type SH3 domain. This is most likely achieved by increasing the population of "binding-competent" conformation by an increased conformational sampling.



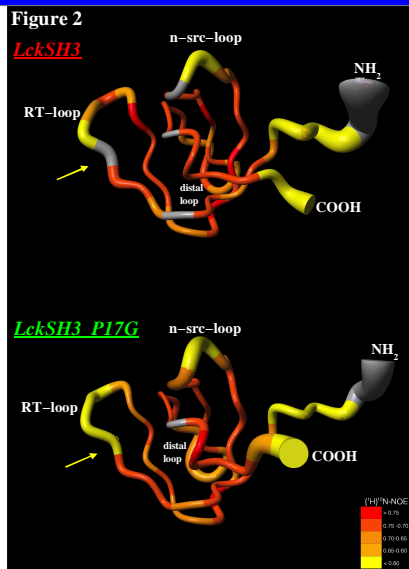
Sequence alignment of the SH3 domains from the tyrosine kinases Lck, Lyn, Hck, Src, Fyn, Yes and Abl and from phosphatidylinositol 3-kinase (PI3K). The numbering scheme of the Lck SH3 domain used in the present study is given at the top. Strictly conserved residues are denoted with an asterisk, and positions with conservative substitutions are denoted with a dot. Elements of secondary structure present in the structure of LckSH3 are given below the alignment. Gray boxes highlight those stretches of amino acids that are known to belong to the canonical binding site of SH3 domains including the RT loop, the n-src loop, and the  $3_{10}$  helix.

### MD simulations

All molecular dynamics simulations were performed using the AMBER 6.0 simulation package and the Cornell et al. force field<sup>11</sup> with the TIP3P water model. For the wild-type LckSH3 six different starting structures, representing the six lowest energy structures of the NMR structure ensemble 1h92<sup>11</sup>, were taken. P17G mutations of these structures were generated using SYBYL6.5 (Tripos Associates Inc., 1998). The molecules were solvated in  $-60 \times 60 \times 60 \text{ \AA}$  waterbox and neutralized by adding counterions. After energy minimization using the SANDER module the temperature of the system was raised gradually from 100 to 300 K, and the system was equilibrated at 300 K for 22.5 ps. An additional 202.5 ps MD simulation was performed for data collection. 135 snapshots were saved for the subsequent analysis, corresponding to a 1.5 ps time step each of the simulation.

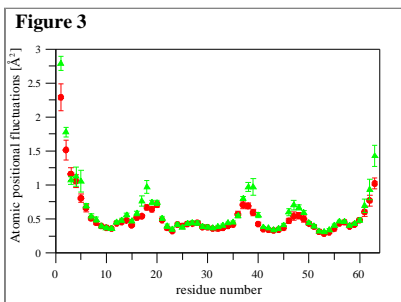


MOLSCRIPT drawing of the LckSH3 domain. The elements of regular secondary structure are emphasized as ribbon representation. The conserved residues that are known to be important for ligand binding are shown as red sticks. Position of residue 17 is marked by a yellow arrow.



MOLMOL representation of the Lck backbone fluctuations observed in the MD simulations. The radius of the tube is drawn proportional to the mean backbone fluctuation. In addition, residues are grouped and color-coded according to the  $\{^1\text{H}\}^{-15}\text{N}$ -NOE value as given in the legend. Position of residue 17 is marked by a yellow arrow.

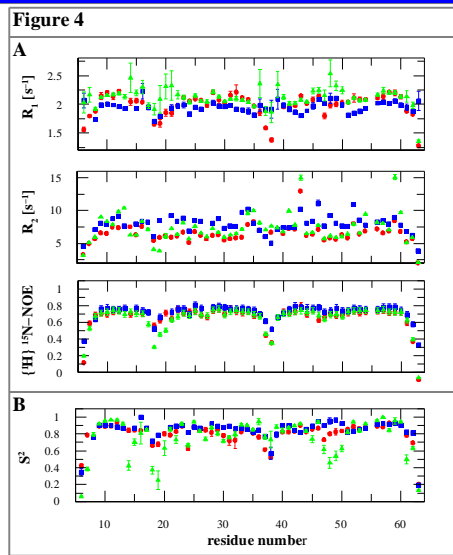
The average (mass-weighted) residual backbone fluctuations are extracted from the trajectory-files using the PTRAJ program in AMBER 6.0. Figure 3 shows the mean values and standard errors of the backbone fluctuation for each residue. The proline to glycine exchange in position 17 increases the fluctuation of almost all amino acids of the RT loop involved in interaction with proline-rich ligands. Likewise, the fluctuation of the n-src loop and the distal loop increases significantly, whereas the elements of regular secondary structure remain unchanged generating a rigid core. The increase of fluctuation of all loops indicates global effects on the conformational stability of the whole domain.



Representation of the atomic positional fluctuation of the backbone (CA, C, and N) during the MD simulation of 200 ps. wild-type LckSH3 (red), LckSH3\_P17G mutant (green)

### NMR-experiments

To extract microscopic parameters of the relaxation rates  $^{15}\text{N}$ - $R_1$ ,  $^{15}\text{N}$ - $R_2$ , and  $\{^1\text{H}\}^{-15}\text{N}$ -NOE (Figure 4A) a Lipari-Szabo analysis was performed with the software package TENSOR2<sup>21</sup>. The comparison of an isotropic diffusion model with a fully anisotropic diffusion model revealed very similar results. Thus the domains were approximated by an isotropic diffusion model and the small amount of anisotropy present in the experimental data is insignificant and can be ignored. For the final fitting, total correlation times ( $\tau_c$ ) of 5.25 ns, 4.62 ns and 5.01 ns for LynSH3, LckSH3 and the LckSH3\_P17G, respectively, were used. The resulting order parameters  $S^2$ , which represent the local rigidity of the structure, are depicted in Figure 4B.  $S^2$  is close to the maximum of 1.0 for the core residues of wild-type LckSH3 and LynSH3, whereas amino acids belonging to the RT loop, n-src loop and to a lesser extent to the distal loop exhibit reduced  $S^2$  values. This finding is in good agreement with the  $\{^1\text{H}\}^{-15}\text{N}$ -NOE for the SH3 domains investigated. The residues of regular secondary structure show values near the maximum theoretical  $\{^1\text{H}\}^{-15}\text{N}$ -NOE of 0.834 (at 60 MHz  $^{15}\text{N}$  NMR frequency) qualitatively reflecting highly restricted internal motion, whereas values smaller than 0.65 (RT loop and n-src loop) are indicative of substantial internal motion on fast time scales (ps–ns).

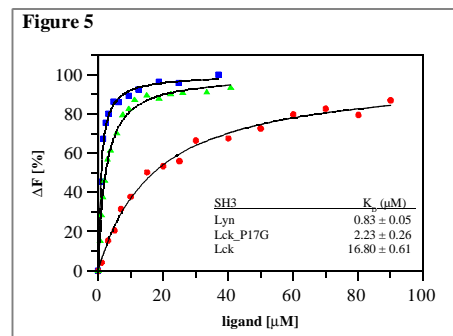


(A)  $^{15}\text{N}$  backbone amide relaxation parameters of LynSH3 (blue), LckSH3 (red) and LckSH3\_P17G (green). From top to bottom: longitudinal relaxation rates ( $R_1$ ), transverse relaxation rates ( $R_2$ ), and  $\{^1\text{H}\}^{-15}\text{N}$ -NOE. (B) Order parameter ( $S^2$ ), representing the local rigidity of the structure, derived from an overall isotropic numbering fit by TENSOR2<sup>21</sup>.

Figure 2 shows the radius of the backbone proportional to the mean fluctuation observed in MD simulations, and the residues color-coded according to the values of the  $\{^1\text{H}\}^{-15}\text{N}$ -NOE. This representation reveals a high correlation between the motions observed in the molecular dynamics calculations and the experimental data. The  $S^2$  profiles are similar for the wild-type LckSH3 and the mutant SH3 except for the loops. It is noteworthy that the lowest  $S^2$  values are to be found in the RT loop and distal loop. Thus the P17G mutant not only causes local effects in the RT loop, but reveals changes throughout the whole domain. This finding is supported by  $\text{D}_2\text{O}$  exchange experiments (data not shown) indicating a dramatic increase of flexibility on the ms to min. time scale for the proline to glycine mutant LckSH3.

### Fluorescence spectroscopy

One of the major differences of the RT loop of LckSH3 and LynSH3 is position 17. Lyn, having a glycine at position 17 binds a 20mer peptide with a low  $K_D$  of 0.8  $\mu\text{M}$ , whereas the  $K_D$  for the Lck-ligand interaction is 16.8  $\mu\text{M}$ . Mutation of proline to glycine increases the affinity of Lck by nearly one order of magnitude ( $K_D$  2.2  $\mu\text{M}$ ) (Figure 5).



Affinity measurements of a 20mer proline-rich peptide (Ac-ATLDPGMP TPPLPRPANLG-Amid) for SH3 domains. Fluorescence titration of LckSH3 (red), LckSH3\_P17G (green), and LynSH3 (blue).

### Conclusion

Usually increased ligand affinity is archived by additional van der Waals or electrostatic interactions. Lck\_P17G reveals an alternative principle. Mutation of proline 17 of the RT loop to glycine increases the  $K_D$  of a 20mer peptide by nearly one order of magnitude. This is most likely achieved by increasing the population of "binding-competent" conformation by an increased conformational sampling.

### References

- Cornell, W.D. et al. (1995). *J. Am. Chem. Soc.* **117**: 5179–97
- Dosset, P. et al. (2000). *J. Biomol. NMR* **16**(1):23–8
- Schweimer, K. et al. (2002). *Biochemistry* **41**(16):5120–30